Reactivation of critical period plasticity in adult auditory cortex through chemogenetic silencing of parvalbumin-positive interneurons

J. Miguel Cisneros-Franco[a,b,1] and Étienne de Villers-Sidani[a,b,1]

[a]Montreal Neurological Institute, McGill University, Montreal, QC H3A 2B4, Canada; and [b]Centre for Research on Brain, Language and Music, McGill University, Montreal, QC H3G 2A8, Canada

Edited by Michael S. Gazzaniga, University of California, Santa Barbara, CA, and approved November 25, 2019 (received for review August 2, 2019)

Sensory experience during early developmental critical periods (CPs) has profound and long-lasting effects on cortical sensory processing perduring well into adulthood. Although recent evidence has shown that reducing cortical inhibition during adulthood reinstates CP plasticity, the precise cellular mechanisms are not well understood. Here, we show that chemogenetic inactivation of parvalbumin-positive (PV^+) interneurons is sufficient to reinstate CP plasticity in the adult auditory cortex. Bidirectional manipulation of PV^+ cell activity affected neuronal spectral and sound intensity selectivity and, in the case of PV^+ interneuron inactivation, was mirrored by anatomical changes in PV and associated perineuronal net expression. These findings underscore the importance of sustained PV-mediated inhibitory neurotransmission throughout life and highlight the potential of chemogenetic approaches for harnessing cortical plasticity with the ultimate goal of aiding recovery from brain injury or disease.

auditory cortex | plasticity | GABA | parvalbumin | perineuronal nets

Parvalbumin-positive (PV^+) cells, the most numerous class of inhibitory interneurons, have been the subject of several neuroplasticity studies as they contribute to both the opening and closing of developmental critical periods (CPs) (1–4). Furthermore, PV^+ cell function and structure are impaired in states of maladaptive plasticity (5, 6), which underlies their importance in health and disease. However, the specific role of PV^+ interneurons in maintaining the stability of sound frequency representations in primary auditory cortex (A1) has not been investigated. To address this gap in knowledge, we first examined the anatomical and functional correlates of PV^+ cell manipulation, and then tested whether silencing of PV^+ cells was sufficient to reinstate CP plasticity in the adult A1. All procedures were approved by the Montreal Neurological Institute Animal Care Committee and follow the guidelines of the Canadian Council on Animal Care.

Results and Discussion

PV is a calcium-buffer protein involved in the modulation of short-term synaptic plasticity (7). Recent studies have uncovered PV expression as a reliable proxy for cellular function and shown that cortical PV staining intensity (SI_{PV}) is correlated with the degree of experience-dependent plasticity (8, 9). Another closely related structure involved in the regulation of plasticity are perineuronal nets (PNNs), a specialized extracellular matrix deposited preferentially around PV^+ cells in an activity-dependent manner (10, 11). Case in point, gamma-aminobutyric acid (GABA) antagonists reactivate CP plasticity and reduce the number of PNNs (12), whereas GABA agonists restore PV/PNN expression and limit plasticity in aged cortex (13).

To determine whether selective manipulation of PV^+ cell activity in A1 might induce a shift in PV/PNN expression, we first transfected PV-Cre rats (Horizon Discovery) with either an inhibitory or excitatory DREADD [pAAV-hSYN-DIO-hM4D(Gi)-mCherry, "PVI" or pAAV-hSYN-DIO-hM3D(Gq)-mCherry, "PVE," respectively; Neurophotonics, QC]. We then measured PV/PNN immunoreactivity upon treatment with clozapine-*N*-oxide (CNO, the DREADD activator) treatment (Fig. 1*A*; detailed experimental protocols can be found at https://doi.org/10.6084/m9.figshare.10248878.v3 (14). In line with previous reports (9, 11), we found a significant effect of condition—naive (Ctrl), PV_I, PV_E—on overall SI_{PV} (Fig. 1*B*). Dividing PV^+ cells in 4 subgroups as a function of SI_{PV} (9, 13) revealed specifically an increase in the proportion of low-intensity PV cells and loss of the high-intensity PV fraction with PV^+ cell inactivation, relative to the PV_E group (Fig. 1*D*). Mirroring these findings, silencing of PV^+ cells was associated with an increase in the low-PNN fraction and a decrease in the high-PNN fraction, relative to Ctrl and PV_E rats (Fig. 1 *C* and *E*). However, we did not observe a significant increase in the high-intensity fractions for either PV or PNN expression upon PV^+ cell activation relative to the Ctrl condition (Fig. 1 *D* and *E*). Although this result is at odds with a previous study using chemogenetics in other (nonsensory) cortical areas (9), it is possible that PV/PNN expression was at or near ceiling, as the adult cortex is characterized by a high basal inhibitory tone that allows for stable sensory representations and high-fidelity discrimination of sensory inputs (3, 4, 12).

By virtue of their numerous electric and chemical connections (15), PV^+ cells inhibit neurotransmission near the site of action potential initiation and exert recurrent and lateral inhibition (6). To test whether PV^+ interneurons specifically modulate A1 receptive field (RF) selectivity—as measured by intensity threshold and bandwidth 20 dB sound pressure level above threshold (BW20)—we recorded A1 tone-evoked potentials in Ctrl and DREADD-transfected rats (PV_I and PV_E, before and after CNO treatment; Fig. 1 *F* and *G*) as described in ref. 16. We found a significant difference in BW20 between the PV_I and PV_E groups upon administration of CNO (Fig. 1*H*). Moreover, increasing PV^+ interneuron activity resulted in higher thresholds relative to both Ctrl and PV_I-CNO rats (Fig. 1*I*). Onset latencies remained unchanged, except for a significant difference between the PV_I-CNO and PV_E-CNO groups (Fig. 1*J*). These results suggest that PV^+ cells exert bidirectional control over both spectral and sound intensity selectivity, providing a mechanistic explanation for the effects on A1 RFs elicited by GABA agonists and antagonists

Author contributions: J.M.C.-F. and E.d.V.-S. designed research; J.M.C.-F. performed research; J.M.C.-F. analyzed data; and J.M.C.-F. and E.d.V.-S. wrote the paper.

The authors declare no competing interest.

Data deposition: Detailed protocols, methods, figures, dataset, and analyses have been deposited in the online open access repository Figshare, https://doi.org/10.6084/m9.figshare.10248878.v3.

[1]To whom correspondence may be addressed. Email: mike.cisneros-franco@mail.mcgill.ca or etienne.de-villers-sidani@mcgill.ca.

This article contains supporting information online at https://www.pnas.org/lookup/suppl/doi:10.1073/pnas.1913227117/-/DCSupplemental.

First published December 16, 2019.

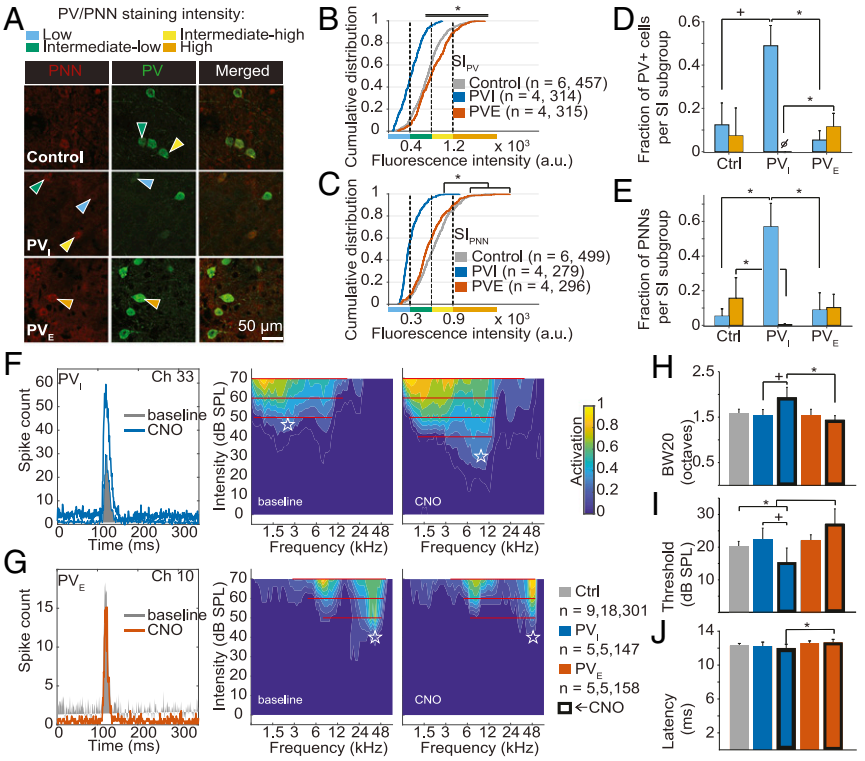

Fig. 1. Effects of PV$^+$ cell manipulation on A1 anatomical and functional properties. Kruskal–Wallis test was used to assess the effect of condition (χ^2 and P value are reported); P values of follow-up pairwise comparisons were corrected with Tukey's post hoc test. (*A*) Microphotographs stained for PV/PNN. Cumulative distribution of (*B*) SI_{PV} [χ^2 (2) = 306.19, $P < 0.001$; all pairwise comparisons, $P \leq 0.004$] and (*C*) SI_{PNN} [χ^2 (2) = 317.7, $P < 0.001$; PV_I vs. PV_E/Ctrl, both $P < 0.001$; control vs. PV_E, $P = 0.39$]. Relative (subgroup analysis) distribution of (*D*) SI_{PV} [low-PV, χ^2 (2) = 8.85, $P = 0.011$, PV_I vs. Ctrl/PV_E, both $P \leq 0.067$, PV_E vs. Ctrl, $P = 0.62$; high-PV, χ^2 (2) = 7.03, $P = 0.029$, PV_I vs. PV_E, $P = 0.022$; all other, $P \geq 0.21$] and (*E*) SI_{PNN} [low-PNN, χ^2 (2) = 8.09, $P = 0.017$, PV_I vs. PV_E/Ctrl, both $P \leq 0.03$, PV_E vs. Ctrl, $P = 0.94$; high-PV, χ^2 (2) = 6.56, $P = 0.037$, PV_I vs. Ctrl, $P = 0.032$; all other, $P \geq 0.17$]. n = number of subjects, number of measurements per group. Examples of peristimulus time histograms (*Left*), and RFs (*Right*) before and after (≥20 min) CNO administration in (*F*) h4MDi- and (*G*) h3MDq-transfected PV-Cre rats. A1 multiunit response properties: (*H*) BW20 [χ^2 (4) = 14.58, $P = 0.0057$; PV_I-CNO vs. PV_E-CNO, $P = 0.0025$, PV_I-CNO vs. PV_I-NaCl, $P = 0.085$, all other, $P \geq 0.13$]. (*I*) Intensity thresholds [χ^2 (4) = 18.21, $P = 0.0011$; Ctrl vs. PV_E-CNO, $P = 0.0191$, PV_I-CNO vs. PV_E-CNO, $P < 0.001$, PV_I-NaCl vs. PV_I-CNO, $P = 0.082$, all other, $P \geq 0.22$]. (*J*) Onset latencies [χ^2 (4) = 10.31, $P = 0.035$; PV_I-CNO vs. PV_E-CNO, $P = 0.038$, all other, $P \geq 0.13$]. n = number of subjects, recording positions, cortical sites per group.

(17). These findings also raise the possibility that reduced PV$^+$ cell function could lead to the instability of sensory representations, as is observed in states of enhanced but maladaptive plasticity associated with reduced intracortical inhibition, such as in autism (5), in aging (13), and following noise exposure (16).

Passive tone exposure (PTE) causes a massive expansion in the proportion of A1 sites tuned to the stimulus frequency, but only during early development (18). To test whether silencing PV$^+$ cells is sufficient to reactivate CP plasticity in A1, we treated PV_I-transfected rats with i.p. CNO (1 mg/kg, b.i.d.) or NaCl (1 mL/kg, b.i.d.) during 7-kHz PTE at 60 dB for 7 d as detailed in ref. 16 (Fig. 2*A*). We assessed both characteristic frequency (CF) and best frequency at 60 dB (BF), as CF describes tuning at threshold intensities, which vary across neurons, whereas BF describes tuning at the exposure intensity (Fig. 2 *B* and *C*). We found a significantly greater percentage of map area tuned to within 1/2 octave of the exposure tone in the CNO-treated group (CF mean ± SEM: exposed, 20.6 ± 4.1%; naive, 3 ± 0.5%; effect size $\eta^2 = 0.29$; BF: exposed, 14.7 ± 1.3%; naive, 6.5 ± 0.6%; $\eta^2 = 0.25$) but not in saline-treated rats (CF, 4.8 ± 1.9%; BF, 9.4 ± 1.3%; Fig. 2 *D* and *E*). Notably, the magnitude and effect size of this intervention on CF representation was comparable to what we have previously observed with PTE during the CP for frequency tuning (exposed, 14.3%; naive, 4.6%; effect size $\eta^2 = 0.25$; original data from ref. 12; see also Dataset S1). These data suggest that PV$^+$ interneurons are indeed necessary for the stability of the A1 frequency tuning map and confirm related findings regarding their role in limiting plasticity elicited by passive experience past the CP (3). Although changes in the representation of both CF and BF are considered an indication of thalamocortical plasticity, the larger shift in CF, relative to BF, observed following PV$^+$ cell inactivation might be explained by the greater natural variability of excitatory–inhibitory balance at threshold levels (19). However, the finding of a significant effect of this intervention on both BF and CF suggests that these changes represent a real shift in RF responsiveness and are not only a consequence of tuning instability.

Our results show that PV$^+$ interneurons regulate the fidelity of sensory representations in the auditory system, both in the short and medium term (minutes and days, respectively). It remains a possibility that, over longer time frames, other regulatory elements of plasticity might compensate for loss of PV-related inhibition (4), thus limiting the plastic changes herein described. Given the prominence of rats as a model for the study of behavior, future studies in

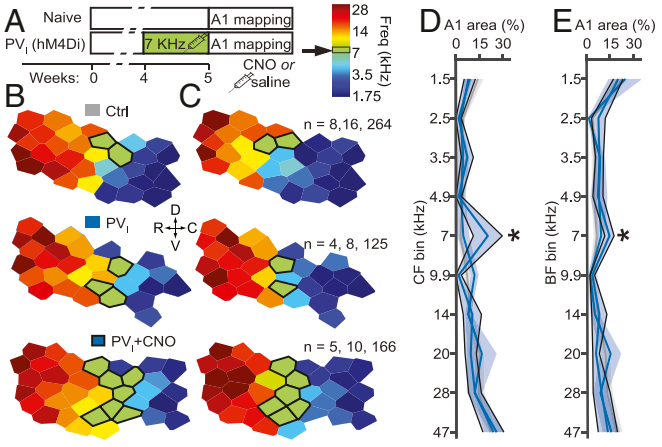

Fig. 2. Silencing of PV$^+$ interneurons reactivates A1 frequency tuning plasticity. (*A*) Experimental timeline. Examples of A1 tuning maps for (*B*) characteristic frequency (CF) and (*C*) best frequency at exposure intensity (BF). Outlined sites are tuned at 7 kHz ± 1/2 octave. All measures were evaluated by 2-way ANOVAs with bin and frequency as factors, followed by simple main effects tests and Tukey's post hoc test for the bins centered on 7 kHz, relative to Ctrl. (*D*) CF. Interaction: both $F_{(9,100)} \geq 2.5$, $P \leq 0.01$; 7-kHz bin: CNO, $P \sim 0$, NaCl ~ 1. (*E*) BF. Interaction: both $F_{(9,100)} \geq 1.8$, $P \leq 0.07$; 7-kHz bin: CNO, $P \sim 0$; NaCl, $P = 0.99$ (Dataset S1). n = number of subjects, recording positions, cortical sites per group.

Cre-transgenic rats may examine the role of PV^+ cells in perceptual learning across sensory systems (6, 9). These will improve our understanding of adult plasticity and help in devising better rehabilitation strategies for patients with perceptual and cognitive impairments (5).

ACKNOWLEDGMENTS. This work was funded by Canadian Institutes of Health Research (CIHR) Grant MOP-133426 (to E.d.V.-S.) and a CIHR Vanier Canada Graduate Scholarship (to J.M.C.-F.). The Centre for Research on Brain, Language and Music is funded by Fonds de Recherche du Québec–Nature et Technologies and Fonds de Recherche du Québec–Société et Culture. We thank L. Ouellet and Y. Chaudron for technical assistance and P. Voss for help with editing.

1. M. Fagiolini *et al*., Specific $GABA_A$ circuits for visual cortical plasticity. *Science* **303**, 1681–1683 (2004).
2. Y. Yazaki-Sugiyama, S. Kang, H. Câteau, T. Fukai, T. K. Hensch, Bidirectional plasticity in fast-spiking GABA circuits by visual experience. *Nature* **462**, 218–221 (2009).
3. S. J. Kuhlman *et al*., A disinhibitory microcircuit initiates critical-period plasticity in the visual cortex. *Nature* **501**, 543–546 (2013).
4. A. E. Takesian, T. K. Hensch, Balancing plasticity/stability across brain development. *Prog. Brain Res.* **207**, 3–34 (2013).
5. O. Marín, Interneuron dysfunction in psychiatric disorders. *Nat. Rev. Neurosci.* **13**, 107–120 (2012).
6. H. Hu, J. Gan, P. Jonas, Interneurons. Fast-spiking, parvalbumin$^+$ GABAergic interneurons: From cellular design to microcircuit function. *Science* **345**, 1255263 (2014).
7. O. Caillard *et al*., Role of the calcium-binding protein parvalbumin in short-term synaptic plasticity. *Proc. Natl. Acad. Sci. U.S.A.* **97**, 13372–13377 (2000).
8. D. Rowlands *et al*., Aggrecan directs extracellular matrix-mediated neuronal plasticity. *J. Neurosci.* **38**, 10102–10113 (2018).
9. F. Donato, S. B. Rompani, P. Caroni, Parvalbumin-expressing basket-cell network plasticity induced by experience regulates adult learning. *Nature* **504**, 272–276 (2013).
10. A. Dityatev *et al*., Activity-dependent formation and functions of chondroitin sulfate-rich extracellular matrix of perineuronal nets. *Dev. Neurobiol.* **67**, 570–588 (2007).
11. E. Favuzzi *et al*., Activity-dependent gating of parvalbumin interneuron function by the perineuronal net protein brevican. *Neuron* **95**, 639–655.e10 (2017).
12. A. Harauzov *et al*., Reducing intracortical inhibition in the adult visual cortex promotes ocular dominance plasticity. *J. Neurosci.* **30**, 361–371 (2010).
13. J. M. Cisneros-Franco, L. Ouellet, B. Kamal, E. de Villers-Sidani, A brain without brakes: Reduced inhibition is associated with enhanced but dysregulated plasticity in the aged rat auditory cortex. *eNeuro* **5**, ENEURO.0051-18.2018 (2018).
14. M. Cisneros-Franco, E. de Villers-Sidani, SI Appendix for Manuscript: Reactivation of critical period plasticity in adult auditory cortex through chemogenetic silencing of parvalbumin-positive interneurons. Figshare. https://doi.org/10.6084/m9.figshare.10248878.v3. Deposited 14 November 2019.
15. M. Galarreta, S. Hestrin, Electrical and chemical synapses among parvalbumin fast-spiking GABAergic interneurons in adult mouse neocortex. *Proc. Natl. Acad. Sci. U.S.A.* **99**, 12438–12443 (2002).
16. M. E. Thomas, N. H. M. Friedman, J. M. Cisneros-Franco, L. Ouellet, É. de Villers-Sidani, The prolonged masking of temporal acoustic inputs with noise drives plasticity in the adult rat auditory cortex. *Cereb. Cortex* **29**, 1032–1046 (2019).
17. Y.-T. Mao, S. L. Pallas, Cross-modal plasticity results in increased inhibition in primary auditory cortical areas. *Neural Plast.* **2013**, 530651 (2013).
18. E. de Villers-Sidani, E. F. Chang, S. Bao, M. M. Merzenich, Critical period window for spectral tuning defined in the primary auditory cortex (A1) in the rat. *J. Neurosci.* **27**, 180–189 (2007).
19. Y. Zhao *et al*., Imbalance of excitation and inhibition at threshold level in the auditory cortex. *Front. Neural Circuits* **9**, 11 (2015).